Residual Data-Driven Variational Multiscale Reduced Order Models for Convection-Dominated Problems ⋆

Birgul Koc * **Samuele Rubino** ** **Tomás Chacón** *** **Traian Iliescu** ****

* *University of Seville, EDAN, Spain (e-mail: bkoc@us.es).*
** *University of Seville, EDAN, Spain (e-mail: samuele@us.es)*
*** *University of Seville, EDAN, Spain (e-mail: chacon@us.es)*
**** *Virginia Tech, USA (e-mail: iliescu@vt.edu)*

1. INTRODUCTION

As a mathematical model, we use Navier-Stokes equations (NSE) (1)-(2):

$$\frac{\partial \boldsymbol{u}}{\partial t} - Re^{-1}\Delta \boldsymbol{u} + \boldsymbol{u}\cdot\nabla\boldsymbol{u} + \nabla p = \boldsymbol{0}\,, \tag{1}$$

$$\nabla\cdot\boldsymbol{u} = 0\,, \tag{2}$$

where $\boldsymbol{u}$ is the velocity, p the pressure, t the continuous time instant, and Re the Reynolds number. Furthermore, we use homogeneous Dirichlet boundary conditions.

We use *proper orthogonal decomposition* (POD) to obtain the *reduced order model* (ROM) basis and operators for all ROMs. Thanks to the orthogonality of the ROM basis functions, we can decompose the ROM space into *large* and *small* spaces as follows: $\boldsymbol{X}^d = \boldsymbol{X}^L \oplus \boldsymbol{X}^S$, where $\boldsymbol{X}^d := \text{span}\{\boldsymbol{\varphi}_1, ..., \boldsymbol{\varphi}_d\}$, $\boldsymbol{X}^L := \text{span}\{\boldsymbol{\varphi}_1, ..., \boldsymbol{\varphi}_L\}$, and $\boldsymbol{X}^S := \text{span}\{\boldsymbol{\varphi}_{L+1}, ..., \boldsymbol{\varphi}_d\}$.

When all the ROM modes are used, the ROM approximation $\boldsymbol{u}_d$, i.e.,

$$\boldsymbol{u}_d = \sum_{j=1}^{d} (\boldsymbol{a}_d)_j\, \boldsymbol{\varphi}_j \tag{3}$$

is the most accurate ROM approximation of the *full order model* (FOM) solution with the given data in the POD sense.

For laminar flows, a low-dimensional ROM solution $\boldsymbol{u}_L$, with small $L \ll d$, yields an accurate approximation of the FOM solution. In the resolved regime, the most straightforward model of ROMs, *Galerkin ROM* (G-ROM) can be used to obtain the ROM solution $\boldsymbol{u}_L$:

$$\dot{\boldsymbol{a}_L} = \boldsymbol{A_{LL}}\,\boldsymbol{a_L} + \boldsymbol{a_L}^\top\,\boldsymbol{B_{LLL}}\,\boldsymbol{a_L}, \tag{4}$$

where $(\boldsymbol{A_{LL}})_{ij} := -Re^{-1}(\nabla\boldsymbol{\varphi}_i, \nabla\boldsymbol{\varphi}_j)$ and $(\boldsymbol{B_{LLL}})_{ijk} := -(\boldsymbol{\varphi}_i, \boldsymbol{\varphi}_j\cdot\nabla\boldsymbol{\varphi}_k)$, respectively, $\forall i,j,k = 1,...,L$. The derivation of the G-ROM (4) is built by replacing $\boldsymbol{u}$ in (1)-(2) with $\boldsymbol{u}_L$ and projecting the resulting system onto the ROM space $\boldsymbol{X}^L$.

However, for turbulent flows, the low-dimensional ROM solution $\boldsymbol{a}_L$ of (4) is not an accurate approximation of the FOM solution. To increase the numerical accuracy of $\boldsymbol{a}_L$ without significantly increasing the computational cost, one needs to add a low-dimensional ROM *closure term* to the G-ROM (4).

⋆

2. ROM CLOSURE MODELS

The ROM closure modeling aims to model the closure term which is derived from a *variational multiscale* (VMS) setting (see Mou et al. (2021) and Ballarin et al. (2020)). To construct the ROM closure term, first, we need to define the large and sub-scale solutions of the most accurate ROM solution, $\boldsymbol{u}_d$, as follows:

$$\boldsymbol{u}_L := \sum_{j=1}^{L} (\boldsymbol{a}_L)_j\, \boldsymbol{\varphi}_j, \qquad \boldsymbol{u}_S := \sum_{j=L+1}^{d} (\boldsymbol{a}_S)_j\, \boldsymbol{\varphi}_j. \tag{5}$$

Then, we obtain the large and sub-scale equations: (i) replace the $\boldsymbol{u}$ in (1)-(2) with $\boldsymbol{u}_d = \boldsymbol{u}_L + \boldsymbol{u}_S$ and project the resulting system onto the ROM spaces $\boldsymbol{X}^L$ and $\boldsymbol{X}^S$, respectively. Then, the large and sub-scale equations are:

$$\begin{aligned}\dot{\boldsymbol{a}_L} &= \boldsymbol{A}_{LL}\boldsymbol{a}_L + \boldsymbol{A}_{LS}\boldsymbol{a}_S + \boldsymbol{a}_L^\top\boldsymbol{B}_{LLL}\boldsymbol{a}_L \\ &\quad + \boldsymbol{a}_L^\top\boldsymbol{B}_{LLS}\boldsymbol{a}_S + \boldsymbol{a}_S^\top\boldsymbol{B}_{LSL}\boldsymbol{a}_L + \boldsymbol{a}_S^\top\boldsymbol{B}_{LSS}\boldsymbol{a}_S, \end{aligned} \tag{6a}$$

$$\begin{aligned}\dot{\boldsymbol{a}_S} &= \boldsymbol{A}_{SS}\boldsymbol{a}_S + \boldsymbol{A}_{SL}\boldsymbol{a}_L + \boldsymbol{a}_S^\top\boldsymbol{B}_{SSS}\boldsymbol{a}_S \\ &\quad + \boldsymbol{a}_S^\top\boldsymbol{B}_{SSL}\boldsymbol{a}_L + \boldsymbol{a}_L^\top\boldsymbol{B}_{SLS}\boldsymbol{a}_S + \boldsymbol{a}_L^\top\boldsymbol{B}_{SLL}\boldsymbol{a}_L. \end{aligned} \tag{6b}$$

In this work, we use two different ROM closure constructions, which yield two different ROM model: the *coefficient-based data-driven variational multiscale* ROM (C-D2-VMS-ROM) and the *residual-based data-driven variational multiscale* ROM (R-D2-VMS-ROM).

The C-D2-VMS-ROM (Mou et al. (2021)) is derived from the large-scale equation (6a) by defining the closure term as "**closure term** $= \boldsymbol{A}_{LS}\boldsymbol{a}_S + \boldsymbol{a}_L^\top\boldsymbol{B}_{LLS}\boldsymbol{a}_S + \boldsymbol{a}_S^\top\boldsymbol{B}_{LSL}\boldsymbol{a}_L + \boldsymbol{a}_S^\top\boldsymbol{B}_{LSS}\boldsymbol{a}_S$". Since the **closure term** is not in a closed form, to close it, we use a quadratic coefficient-based ansatz (Mou et al. (2021)), which depends on the large-scale solution $\boldsymbol{a}_L$: "**ansatz** $= \widetilde{\boldsymbol{A}}_{LL}\,\boldsymbol{a}_L + \boldsymbol{a}_L^\top\,\widetilde{\boldsymbol{B}}_{LLL}\boldsymbol{a}_L$".

In the new R-D2-VMS-ROM, we define the closure term and residual-based ansatz from the sub-scale equation (6b) as "**closure term** $= \boldsymbol{a}_S$" and "**ansatz** $= \widetilde{\boldsymbol{A}}_{SS}\,\mathbf{ResS}(\boldsymbol{a}_L) + \mathbf{ResS}(\boldsymbol{a}_L)^\top\,\widetilde{\boldsymbol{B}}_{SSS}\mathbf{ResS}(\boldsymbol{a}_L)$", where the residual is $\mathbf{ResS}(\boldsymbol{a}_L) := \boldsymbol{A}_{SL}\boldsymbol{a}_L + \boldsymbol{a}_L^\top\boldsymbol{B}_{SLL}\boldsymbol{a}_L$.

DOI: 10.34726/9005

To find the unknown operators $\widetilde{\boldsymbol{A}}, \widetilde{\boldsymbol{B}}$, we use a *data-driven* (D2) approach (Rebollo and Coronil (2024)). We obtain the D2 operators by solving the following minimization problem:

$$\min_{\widetilde{\boldsymbol{A}},\widetilde{\boldsymbol{B}}} \sum_{k=1}^{M} \|\mathbf{closure\ term}(\boldsymbol{a}_L^k, \boldsymbol{a}_S^k) - \mathbf{ansatz}(\boldsymbol{a}_L^k)\|_{\mathcal{L}^2}^2, \quad (7)$$

where M represents the number of snapshots. By using the closure terms and ansatzes for the C-D2-VMS-ROM and R-D2-VMS-ROM, we solve (7) to obtain the corresponding D2 operators, i.e. $\widetilde{\boldsymbol{A}}$ and $\widetilde{\boldsymbol{B}}$. Then, by plugging the resulting ansatzes into (6a), C-D2-VMS-ROM and R-D2-VMS-ROM read as follows:

$$\dot{\boldsymbol{a}_L} = (\boldsymbol{A}_{LL} + \widetilde{\boldsymbol{A}}_{\boldsymbol{LL}})\boldsymbol{a}_L + \boldsymbol{a}_L^\top(\boldsymbol{B}_{LLL} + \widetilde{\boldsymbol{B}}_{\boldsymbol{LLL}})\boldsymbol{a}_L, \quad (8a)$$

$$\dot{\boldsymbol{a}_L} = \boldsymbol{A}_{LL}\boldsymbol{a}_L + \boldsymbol{a}_L^\top \boldsymbol{B}_{LLL}\boldsymbol{a}_L + \boldsymbol{A}_{LS}\boldsymbol{a}_S^* + \boldsymbol{a}_L^\top \boldsymbol{B}_{LLS}\boldsymbol{a}_S^* + (\boldsymbol{a}_S^*)^\top \boldsymbol{B}_{LSL}\boldsymbol{a}_L + (\boldsymbol{a}_S^*)^\top \boldsymbol{B}_{LSS}\boldsymbol{a}_S^*, \quad (8b)$$

where approximated sub-scale coefficient $\boldsymbol{a}_S^*$ is computed as $\boldsymbol{a}_S^* := \widetilde{\boldsymbol{A}}_{SS}\,\mathbf{ResS}(\boldsymbol{a}_L) + \mathbf{ResS}(\boldsymbol{a}_L)^\top\, \widetilde{\boldsymbol{B}}_{SSS}\mathbf{ResS}(\boldsymbol{a}_L)$.

3. NUMERICAL RESULTS

We investigate the numerical accuracy of G-ROM, C-D2-VMS-ROM, and new R-D2-VMS-ROM in the numerical simulation of a 2D channel flow past a circular cylinder at Reynolds numbers Re $= 1000$. We present the numerical accuracy of the ROM models for two different regimes: (i) **reconstructive regime**: we build the ROM basis and operators, and D2 operators by using the FOM snapshots from $t = 13$ to $t = 16$. Then, we test ROMs over the same time interval. (ii) **predictive regime**: we build the ROM basis and operators by using the FOM snapshots from $t = 13$ to $t = 16$, and D2 operators by using the FOM snapshots from $t = 13$ to $t = 13.134$. Then, we test ROMs over the longer time interval, $t = 16$ to $t = 23$.

Furthermore, in our numerical accuracy investigation of the ROMs, we use the average $\mathcal{L}^2$ projection error:

$$\mathcal{E}_{avgL^2proj} = \frac{1}{M}\sum_{k=1}^{M}\left\| \boldsymbol{u}_L(t_k) - \sum_{i=1}^{L}\left(\boldsymbol{u}^{FOM}(t_k), \boldsymbol{\varphi}_i\right)\boldsymbol{\varphi}_i \right\|_{\mathcal{L}^2}. \quad (9)$$

In Tables 1-2, we list the average $\mathcal{L}^2$ projection errors of G-ROM, C-D2-VMS-ROM, and R-D2-VMS-ROM for the reconstructive and predictive regimes, respectively. In Table 1, we observe that C-D2-VMS-ROM and R-D2-VMS-ROM yield much better accuracy (for some values, the improvement is more than 2 orders of magnitude) than G-ROM in the reconstructive regime. C-D2-VMS-ROM and R-D2-VMS-ROM have similar accuracy behavior. In Table 2, we still observe that C-D2-VMS-ROM and R-D2-VMS-ROM yield much better accuracy (for some values, the improvement is more than 1 order of magnitude) than G-ROM in the predictive regime. Furthermore, R-D2-VMS-ROM yields better accuracy than C-D2-VMS-ROM.

In Figures 1-2, we plot the kinetic energy of the FOM projection, G-ROM, C-D2-VMS-ROM, and R-D2-VMS-ROM for the reconstructive and predictive regimes, respectively. We fix the large-scale ROM dimension $L = 6$, to compare the kinetic energy behavior of C-D2-VMS-ROM and R-D2-VMS-ROM. We observe that R-D2-VMS-ROM is significantly more accurate than C-D2-VMS-ROM, especially in the predictive regime.

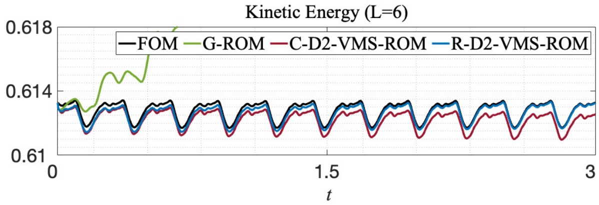

Fig. 1. Reconstructive regime; kinetic energy of ROMs.

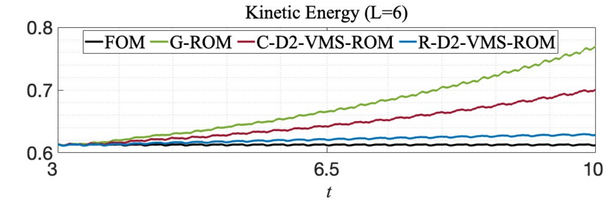

Fig. 2. Predictive regime; kinetic energy of ROMs.

Acknowledgments: Research is partially funded by the Spanish Research Agency Juan de la Cierva 2022 with 2023/1061 and PID2021-123153OB-C21 - Feder Fund Grants.

REFERENCES

Ballarin, F., Rebollo, T.C., Avila, E.D., Mármol, M.G., and Rozza, G. (2020). Certified reduced basis vms-smagorinsky model for natural convection flow in a cavity with variable height. *Computers & Mathematics with Applications*, 80(5), 973–989.

Mou, C., Koc, B., San, O., Rebholz, L.G., and Iliescu, T. (2021). Data-driven variational multiscale reduced order models. *Computer Methods in Applied Mechanics and Engineering*, 373, 113470.

Rebollo, T.C. and Coronil, D.F. (2024). Data-driven stabilized finite element solution of advection-dominated flow problems. *Mathematics and Computers in Simulation*, 226, 540–559.

Table 1. Reconstructive regime; average $\mathcal{L}^2$ projection error (9) for different L values.

L	G-ROM	C-D2-VMS-ROM	R-D2-VMS-ROM
2	4.94e-01	4.00e-03	5.06e-03
3	5.11e-01	3.09e-03	4.17e-03
4	5.98e-01	2.89e-03	1.45e-03
5	6.58e-01	6.07e-03	1.31e-03
6	1.50e-01	2.62e-03	9.83e-04
7	1.36e-01	2.76e-03	4.42e-03
8	7.08e-02	3.14e-03	1.32e-03

Table 2. Predictive regime; average $\mathcal{L}^2$ projection error (9) for different L values.

L	G-ROM	C-D2-VMS-ROM	R-D2-VMS-ROM
2	1.15e+00	4.11e-01	3.59e-01
3	9.22e-01	5.51e-01	6.16e-02
4	7.21e-01	1.98e-01	1.18e-01
5	7.28e-01	5.81e-01	3.11e-01
6	3.54e-01	1.48e-01	4.36e-02
7	3.02e-01	2.81e-01	5.29e-02
8	1.59e-01	9.44e-02	2.53e-02

DOI: 10.34726/9005